

Clustering by soft-constraint affinity propagation: Applications to gene-expression data

Michele Leone^a, Sumedha^a, Martin Weigt^{a1}

^{1a}*Institute for Scientific Interchange, Viale Settimio Severo 65, Villa Gualino, I-10133 Torino, Italy.*

Motivation: Similarity-measure based clustering is a crucial problem appearing throughout scientific data analysis. Recently, a powerful new algorithm called Affinity Propagation (AP) based on message-passing techniques was proposed by Frey and Dueck [1]. In AP, each cluster is identified by a common exemplar all other data points of the same cluster refer to. Since the exemplars in AP are themselves data points, they have to refer to themselves. Albeit its proved power, AP in its present form suffers from a number of drawbacks. The hard constraint of having exactly one exemplar in each cluster restricts the applicability of AP to classes of regularly shaped clusters, and leads to suboptimal performance, *e.g.*, in analyzing gene expression data. This limitation can be overcome by a straight-forward generalization of AP.

Results: By relaxing the AP hard constraints, we introduce a parameter controlling the algorithm's greediness. This parameter controls the importance of the constraints compared to the aim of maximizing the overall similarity, and allows to interpolate between the simple case where each data point selects its closest neighbor as an exemplar and the original AP. The resulting soft-constraint affinity propagation (SCAP) becomes more informative, accurate and leads to more stable clustering. It is easier to interpret the statistical meaning of the tuning process. Even though a new *a priori* free-parameter is introduced, the overall dependence of the algorithm on external tuning is reduced, as robustness is increased and an optimal strategy for parameter selection emerges more naturally. SCAP is tested on biological benchmark data, including in particular microarray data related to various cancer types. We show that the algorithm efficiently unveils the hierarchical cluster structure present in the data sets.

*Contact:*leone,sumedha,weigt@isi.it

I. INTRODUCTION

Clustering based on a measure of similarity is a crucial problem which appears throughout scientific data analysis. For an overview see [3].

Recently, a powerful algorithm called Affinity Propagation (AP) based on *message passing* was proposed by Frey and Dueck [1]. As reported impressively in the original publication, this algorithm achieves a considerable improvement over standard clustering methods like K-means [4], spectral clustering [5] and super-paramagnetic clustering [6, 7].

Based on an *ad hoc* pairwise similarity function between data points, AP seeks to identify each cluster by one of its elements, the so-called *exemplar*. Each point in the cluster refers to this exemplar, and each exemplar is required to refer to itself as a self-exemplar. This hard constraint forces clusters to appear as stars of chemical radius one: There is only one central node, and all other nodes are directly connected to it. AP seeks at maximizing the overall similarity of all data points to their exemplars. The solution to this hard combinatorial task is approximated recursively by sending real-valued messages between data points and constraints, following the ideas of belief-propagation [9, 10]. One of the important points of AP is its computational efficiency: whereas a naive implementation of belief propagation for N data points leads to $O(N^3)$ messages which have to be determined self-consistently, the elegant formulation of Frey and Dueck allows to work with $O(N^2)$ messages only. Therefore the algorithm is feasible even in the presence of very large data sets.

Albeit its impressive power in a wide range of applications [1], AP in its present form suffers from a number of drawbacks. The most important ones related to the present work are[20]:

- The hard constraint in AP relies strongly on *cluster-shape regularity*: Elongated or irregular multi-dimensional data might have more than one simple cluster center. The choice of single exemplars may force division of single clusters into separate subclusters.
- Since all data points in a cluster must point to the same exemplar, all information about both the *internal structure* and the *hierarchical merging/dissociation* of clusters is lost.
- AP has *robustness limitations*: A small perturbation of (self)-similarities (for the definition and significance of self-similarities see the next section) may influence the choice of one or few exemplars, and the hard constraint may trigger an avalanche leading to a different partitioning of the data set into clusters. This point is particularly important in the presence of noise in the data as, *e.g.*, in microarray measurements.

- AP forces each exemplar to point to itself. Why should this be the case? A relaxation of the hard constraint may allow for cluster structures including *second- or higher-order pointing processes*.

These problems may be solved by modifying the original optimization task of AP. As a first step we relax the hard constraint that each exemplar has to be a self-exemplar by introducing a finite penalty term for each constraint violation. This softening can be chosen in a way that the computational complexity of the algorithm remains unchanged, but its performance on biological test sets is improved considerably. Moreover, relaxing the constraint helps in gaining valuable insight into the hierarchical structure of the clustering, increasing result robustness at the same time. By tuning the cluster number we see the merging of two clusters into a single one, or the dissociation of single clusters into two separated ones.

In this work, we first introduce the modifications leading to SCAP. Then we apply it to various biological test data sets. In the methods section we provide a detailed derivation of the algorithm starting from the original optimization task.

II. THE ALGORITHM

Given a set $D = \{x_\mu\}_{\mu=1}^N$ of N data points, the original algorithm of Frey and Dueck takes as input a collection of real valued similarities $S(\mu, \nu)$ between the pairs x_μ, x_ν , $\mu, \nu \in \{1, \dots, N\}$. The choice of the similarity measure is heuristic, non univocal and suggested by the nature of data to be clustered. In the case of high-dimensional data as present in gene-expression analysis, similarity may be measured by the Pearson correlation coefficient or the negative pairwise Euclidean distance. However, for the algorithm described below it is not even necessary that the similarities are symmetric.

The algorithm searches for a mapping $\mathbf{c} : \{1, \dots, N\} \mapsto \{1, \dots, N\}$ which maps each data point μ to its exemplar c_μ which itself is a data point. This mapping shall minimize the cost function (or energy)

$$E_1[\mathbf{c}] = - \sum_{\mu=1}^N S(\mu, c_\mu) \quad (1)$$

which equals minus the overall similarity of the data points to their exemplars. In the original AP algorithm \mathbf{c} is restricted by N hard constraints: Whenever a data point is selected as an exemplar by another data point, it has to be its own self-exemplar.

In this setting, we also need to specify the self-similarities $S(\mu, \mu)$. They describe the availability of data points for being self-exemplars (and thus to serve as a cluster center). Since all data points are *a priori* equally suitable to play such a role, one is naturally led to choose all self-similarities to have some common value $S(\mu, \mu) \equiv -\sigma$, $\mu = 1, \dots, N$. [21] The free model parameter σ acts like a chemical potential in statistical physics, setting the prior likelihood of the number of self exemplars (and of separated clusters consequently). For very small value of σ (value $-\sigma$ larger than all the pair similarities), every data point prefers to be its own exemplar, and the number of clusters equals the number of data points. In the opposite extreme case of large σ (value $-\sigma$ smaller than all the pair similarities), self-exemplars have high cost in Eq. (1), and only a single self-exemplar is allowed for: All data points are collected in one large cluster. For intermediate values σ acts as a tuning parameter for the cluster number which decreases monotonously with σ . Frey and Dueck argue that, if the data set has some underlying structure, the correct clustering can be identified by a comparably broad range of values of the self-similarity in which the inferred cluster structure does not change. If data are not sparse and clusters are symmetrically shaped, then affinity propagation works very well and produces the correct clustering in a very short time.

Finding the cost minimum of $E_1[\mathbf{c}]$ subject to the self-exemplar constraint is a computationally hard task. It can be achieved exactly only for very small systems. The central idea of AP is therefore to identify the exemplars using message passing (belief propagation) as a heuristic strategy [9]: Real-valued messages between pairs of data points are updated recursively until a stable clustering emerges. The original AP equations are a direct application of belief propagation (or, equivalently, the Max-Sum algorithm [10]) to the specific problem under consideration.

There are two types of messages exchanged between data points [1]: The first one is the *responsibility* $r(\mu, \nu)$, sent from data point μ to candidate exemplar ν ; it reflects the accumulated evidence that μ chooses ν as its cluster exemplar. The second message is the *availability* $a(\mu, \nu)$, sent from candidate exemplar ν to datum μ ; it reflects the appropriateness for ν to be an exemplar for μ as a result of the self-exemplar constraint. As mentioned before, the original AP imposes a hard constraint on the exemplars to be self-exemplars. We modify the algorithm of Frey and Dueck by softening the hard constraint on the choice of exemplars. We write the constraint attached to a given data

point μ as follows, with $p \in [0, 1]$:

$$\chi_{\mu}^{(p)}[\mathbf{c}] = \begin{cases} p & \text{if } \exists \nu : c_{\nu} = \mu, c_{\mu} \neq \mu \\ 1 & \text{else.} \end{cases} \quad (2)$$

The first case assigns a penalty p if data point μ is chosen as an exemplar by some other data point ν , without being a self-exemplar. The hard-constraint limit of Frey and Dueck is recovered by setting p to zero. For $p = 1$, $\chi_{\mu}^{(p)}[\mathbf{c}]$ becomes identically one, the minimization task of Eq. (1) becomes unconstrained and independent for all data points, thus each data point chooses his nearest neighbor as an exemplar. An intermediate value of p allows to interpolate between these two extreme cases, and, as we will show via applications on biological data, frequently presents a compromise between the minimization of $E_1[\mathbf{c}]$ on one hand, and the search for compact, robust clusters on the other hand.

Finally we have to introduce a positive real-valued parameter β which weighs the relative importance of the cost minimization with respect to the constraints. In a statistical-physics perspective, this parameter can be seen as a formal inverse temperature. Its introduction allows us to define the probability of an arbitrary clustering \mathbf{c} as

$$P[\mathbf{c}] = \frac{1}{Z} \exp(-\beta E_1[\mathbf{c}]) \prod_{\mu} \chi_{\mu}^{(p)}[\mathbf{c}] \quad (3)$$

$$Z = \sum_{\tilde{\mathbf{c}}} \exp(-\beta E_1[\tilde{\mathbf{c}}]) \prod_{\mu} \chi_{\mu}^{(p)}[\tilde{\mathbf{c}}]$$

where the sum in the partition function Z runs over all mappings $\tilde{\mathbf{c}} : \{1, \dots, N\} \mapsto \{1, \dots, N\}$. In this setting, both clusterings of non-optimal cost and of many violated self-exemplar constraints are suppressed exponentially. The task of finding high-scoring \mathbf{c} can be understood as a minimization problem with the modified cost function

$$E_p[\mathbf{c}] = - \sum_{\mu=1}^N S(\mu, c_{\mu}) - \frac{1}{\beta} \sum_{\mu=1}^N \ln(\chi_{\mu}^{(p)}[\mathbf{c}]) \quad (4)$$

The original AP algorithm is recovered by taking $p = 0$ since any violated constraint sets $P[\mathbf{c}]$ to zero in Eq. (3). For general p , the optimal clustering \mathbf{c}^* can be determined component-wise by maximizing the marginal probabilities,

$$c_{\mu}^* = \operatorname{argmax}_{c_{\mu}} P_{\mu}(c_{\mu}) = \operatorname{argmax}_{c_{\mu}} \sum_{\{c_{\nu}; \nu \neq \mu\}} P[\mathbf{c}] \quad (5)$$

for all data points μ . The exact sum contains N^{N-1} terms, but it can be approximated via belief propagation, see Sec. IV for details.

A. The SCAP equations

In the limit $\beta \rightarrow \infty$, Eq. (3) becomes concentrated to the true cost minima. Looking at Eq. (4) it becomes obvious that a non-zero p in this limit has to scale as $p \propto e^{-\beta \tilde{p}}$ in order to have some non-vanishing contribution. In this limit, we find the SCAP equations (with $\mu \neq \nu$, see again Sec. IV):

$$\begin{aligned} r(\mu, \nu) &= S(\mu, \nu) - \max_{\lambda \neq \nu} [S(\mu, \lambda) + a(\mu, \lambda)] \\ r(\mu, \mu) &= \max[-\tilde{p}, S(\mu, \mu) - \max_{\lambda \neq \mu} \{S(\mu, \lambda) + a(\mu, \lambda)\}] \\ a(\mu, \nu) &= \min\left[0, r(\nu, \nu) + \sum_{\lambda \neq \mu} \max(0, r(\lambda, \nu))\right] \\ a(\mu, \mu) &= \min\left[\tilde{p}, \sum_{\lambda \neq \mu} \max\{0, r(\lambda, \mu)\}\right]. \end{aligned} \quad (6)$$

These $2N^2$ equations are closed and can be solved iteratively. Following Eq. (5) the exemplar c_{μ}^* of any data point μ after convergence of Eqs. (6) can be computed by maximizing the marginal a posteriori probability (given by the sum of responsibility and availability):

$$c_{\mu}^* = \operatorname{argmax}_{\nu} [a(\mu, \nu) + r(\mu, \nu)] \quad (7)$$

Compared to the original AP equations, SCAP amounts to nothing but an additional threshold on the self-availabilities $a(\mu, \mu)$ and the self-responsibilities $r(\mu, \mu)$: For small enough \tilde{p} , $a(\mu, \mu) \rightarrow \tilde{p}$ in many cases, up to $p = 1$ (or $\tilde{p} = 0$), where every site chooses its best first neighbor as its exemplar. \tilde{p} is the interpolating parameter. At the same time, beyond a certain threshold the self responsibility $r(\mu, \mu)$ is substituted with $-\tilde{p}$. For $\tilde{p} \rightarrow \infty$ (*i.e.* $p = 0$) the original AP equations are recovered.

In practice, this means that variables are discouraged to be self exemplars beyond a give threshold, even in the case someone is already pointing at them. The resulting clustering is more stable and obviously allows for a hierarchical structure where λ can point to μ that can point to ν etc. Also loops are possible. In most of the tests performed (both on artificial and biological cancer data) clusters are almost tree-like besides a dimer.

As we change \tilde{p} we go from the naive affinity measure to the greedy limit of the Frey *et al.* algorithm. \tilde{p} plays the role of keeping a check on the greediness introduced. Also, at the same time, via \tilde{p} we get a better view of the hierarchal structure of the clusters. This gives a clear idea of how the clusters were formed and insight on which patterns are wrongly classified and why. Such information is completely lost in the limit $\tilde{p} \rightarrow \infty$.

B. Efficient implementation of the algorithm

The iterative solution of Eqs. (6) can be implemented in the following way:

1. Choose an appropriate similarity measure and assign similarities $S(\mu, \nu)$ for each set of data points. Choose the values of the self-similarity σ and of the constraint strength \tilde{p} .
2. Initialize all $a(\mu, \nu) = r(\mu, \nu) = 0$
3. For all $\mu \in \{1, \dots, N\}$, first update the N responsibilities $r(\mu, \nu)$ and then the N availabilities $a(\nu, \mu)$, using Eqs. (6).
4. Identify the exemplars c_μ by looking at the maximum value of $r(\mu, \nu) + a(\mu, \nu)$ for given μ , according to Eq. (7).
5. Repeat steps 3-4 till there is no change in exemplars for a large number of iterations (we used 10-100 iterations).

Two notes are necessary at this point:

- Step 3 is formulated as a sequential update: For each data point μ , all outgoing responsibilities and then all incoming availabilities are updated before moving to the next data point. This is different from the parallel update with damping suggested by Frey and Dueck in [1]. In numerical experiments we have observed that the sequential update converges faster and in a larger parameter range than the parallel update.
- The naive implementation of the update equations (6) requires $2N^2$ updates, each one of computational complexity $O(N)$. A global update would thus result in a total complexity of $O(N^3)$. A factor N can be gained by first computing the unrestricted max and sum once for a given μ , and than implying the restriction only inside the internal loop over ν . Like this, the total complexity of a global update is $O(N^2)$ and thus feasible even for very large data sets.

In the next section we give the results of the application of the modified AP algorithm to some real data. The preliminary trend shows an increase of robustness, less need of parameter fine-tuning and better number of clusters prediction by SCAP as compared to AP.

III. APPLICATION TO BIOLOGICAL DATA

A. Iris data

The data consist of measurements of sepal length, sepal width, petal length and petal width, performed for 150 flowers, chosen from three species of the flower Iris. It is a benchmark problem for clustering [8]. With a method like super-paramagnetic clustering, the authors were able to cluster 125 of the data points correctly, leaving 25 points unclustered [6]. Note that this method can be formulated efficiently within a message-passing framework as well [7].

When we apply the original AP on Iris data, we can classify the three clusters making 16 errors. With SCAP, we can classify them with just nine errors. We use the Manhattan distance measure for the similarity function, *i.e.* $S(\mu, \nu) = -\sum_{i=1}^4 |x_\mu^i - x_\nu^i|$.

We saw that the points of species *Iris Setosa* separate without any errors. On increasing the value of \tilde{p} , the *Iris Setosa* cluster stays intact and the clusters for *Versicolor* and *Virginica* merge with each other, reflecting the fact that they are closer to each other than to *Setosa*. The errors occur because some samples from these species were closer to samples from other species than to their own.

B. Brain cancer data

We used a test data set monitoring the expression levels of 5597 genes for 42 patients, which was previously correctly classified into 5 diagnosis types by an *a posteriori* assessment method [11]. The data was normalized to mean zero and variance one. In fact, we used the data preprocessed in [12]. A simple Euclidean measure setting the similarity function was used, $S(\mu, \nu) = -\sqrt{\sum_{i=1}^{5597} (x_{\mu}^i - x_{\nu}^i)^2}$. Due to the normalization procedure, this similarity function carries exactly the same information as the Pearson correlation coefficient. The diagnosis information was not used during the clustering, but only for checking the algorithmic outcome.

1. Imposing five clusters in AP and SCAP:

Since we knew that the correct clustering was to identify five different patterns, our first approach was to tune σ and \tilde{p} in order to get five clusters. First, we fixed \tilde{p} to infinity (original AP) and changed σ finding around $\sigma = 70$ the desired number of 5 clusters with 8 errors. The error was calculated *a posteriori* by counting every data point which referring to an exemplar of a different diagnosis. Next we fixed σ to a sufficiently large value (the result becomes insensitive on σ once the latter takes large values), and we changed \tilde{p} . In this case, for $\tilde{p} = 4$ we got 5 clusters with 7 errors. Note that in both cases all errors occur in the last cluster: samples supposed to take diagnosis 5 rarely find an exemplar of the same class. Instead they distribute over the other four diagnoses.

2. Clustering with AP:

Then, instead of fixing the number of clusters, we changed σ continuously for $\tilde{p} \rightarrow \infty$. We counted the number of clusters and of errors as a function of σ , see Fig. 1. The algorithm ground state (configuration of maximum marginals values) in the limit of $\sigma \rightarrow \infty$ is a single cluster.

The first non trivial clustering occurs when the number of clusters remain unchanged for a stable range of σ values. In this preliminary study, we took that to be the actual predicted data clustering. Hence, by looking at Fig. 1, we would conclude that there are three well-distinguishable clusters in the present data set. Look, however, to the number of errors: It is found to be 14-15 in this range, basically due to the wrong assignment of two entire classes to only three exemplars. Four or five clusters can be imposed and lead to lower error values, but require fine-tuning of σ .

3. Clustering with SCAP:

We then fix σ to be very large and change only \tilde{p} . For \tilde{p} we start with seven clusters, but this number decreases rapidly as \tilde{p} increases, see Fig. 2. As before, the point at which the number of clusters is robust against changes in \tilde{p} was taken as the best SCAP clustering. From Fig. 2 we conclude that SCAP identifies 4 clusters. The number of errors in classification is 8. Let us show in more detail how the clusters look as we change the \tilde{p} .

At $\tilde{p} = 0$, the constraint is completely relaxed and every data point chooses its first neighbor as its exemplar (*i.e.* the most similar one to the data point under consideration according to the function S). Look at Figs. 3 to 7 for the change in the clustering number and structure as we increase \tilde{p} . The grey scale of the nodes represents different diagnosis. Data points between (0-9), (10-19), (20-29), (30-33) and (34-41) had same diagnosis. Clearly right from $\tilde{p} = 0$, we see that the last set (34-41) is mixed up with other clusters. At $\tilde{p} = 5$, the data clusters into five groups. Here, groups (0-9), (20-29) and (30-33) have already merged, while (10-19) is still split into two clusters. On the other hand, the points which should have been included in the last cluster (34-41) are distributed among all the others. For $\tilde{p} = 8$ and 10, we see four clusters, errors occurring only in the assignment of points 34 – 41. Most of them seem to belong to group (10-19), suggesting that they have similar expressions. Our conclusion of the previous section, that the data set has only 4 distinguishable clusters, is coherent with this alternative presentation. As we change \tilde{p} , we

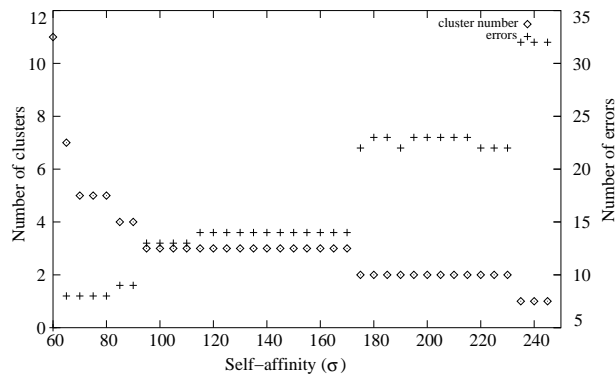


FIG. 1: Plot of number of clusters as a function of self-affinity $S(\mu, \mu) \equiv -\sigma$, for $\tilde{p} = \infty$ (the original AP algorithm). Based on this we would conclude that the data has three nontrivial clusters.

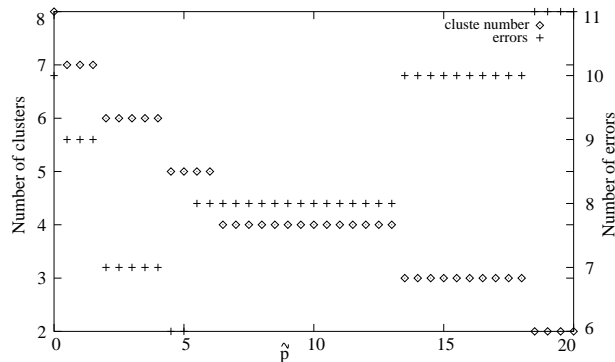


FIG. 2: Plot of number of cluster and errors of SCAP as a function of cutoff parameter \tilde{p} . This plot suggests that the data has four clusters.

can get a possible hierarchal picture of the clusters forming process. As we go to even higher \tilde{p} , we see that groups (0-9) and (30-33) merge, implying that these two are closer together than the rest.

Note that SCAP also provides information about the internal organization inside the clusters. We find, *e.g.*, that the misclassified patterns are always peripheral cluster elements. No other data point refers to them. This information is lost in AP: We show in Fig. 8 the graphical structure of the data-exemplar mapping for original AP. Due to the hard constraint all points belonging to the same cluster refer to the same exemplar, and information about the internal cluster structure is not contained in \mathbf{c}^* .

Another interesting point comes from the comparison of our clustering results with the supervised classification results of [12]. There, a number of state-of-the-art classification algorithms is applied, with training sets containing 2/3, test sets containing 1/3 of the data points. Dettling finds that the minimal generalization error made is 23.8%, corresponding to ca. 10 errors on a data set of cardinality 42. It is interesting to note that SCAP in the clustering corresponding to 4 clusters makes only 8 errors. Note that training in [12] is done on a subset of patterns, but supervision in this case seems to add no valuable information to the unsupervised clustering results.

C. Lymphoma cancer data

We used a data set of 62 patients for 4026 genes, showing 3 different diagnosis [13].

In the limit of \tilde{p} going to infinity, we find the first nontrivial clustering for σ between 150 – 250. In this regime AP group data into 3 sets, making with 3 error. For very high σ and varying \tilde{p} , the 3-groups clustering becomes more stable and robust, while the algorithm makes just one assignment prediction error. In this case, Dettling finds a minimal generalization error of 0.95%, corresponding to less than one error in 62 patterns. Supervision adds some information, even if clustering itself makes only one error.

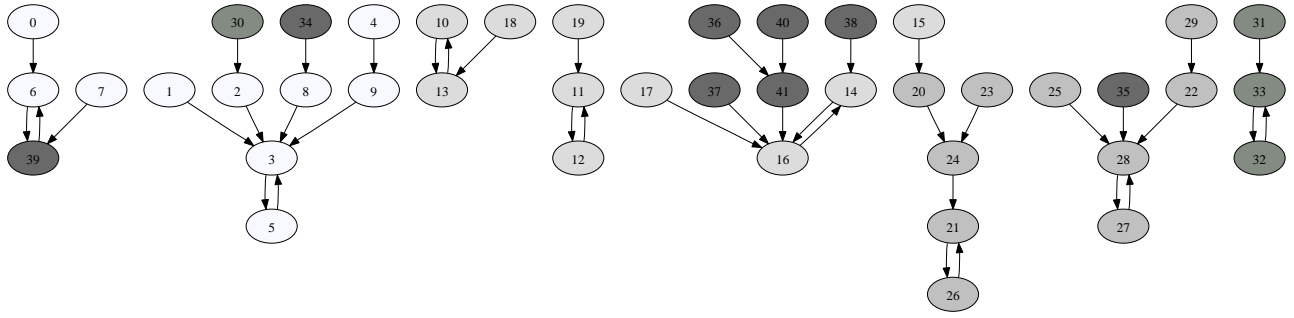


FIG. 3: Graphical presentation of clusters at $\tilde{\rho} = 0$. At this value of $\tilde{\rho}$, data points refer to their nearest neighbor. One can already see that some points corresponding to last diagnosis (points 34-41) are very close to points 10-19.

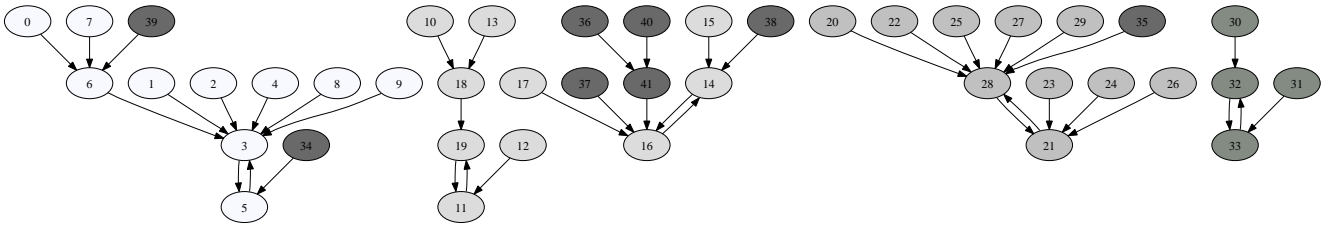


FIG. 4: Graphical presentation of clusters at $\tilde{\rho} = 5$. At this point the data set (0-9),(20-29) and (30-33) are already clustered together

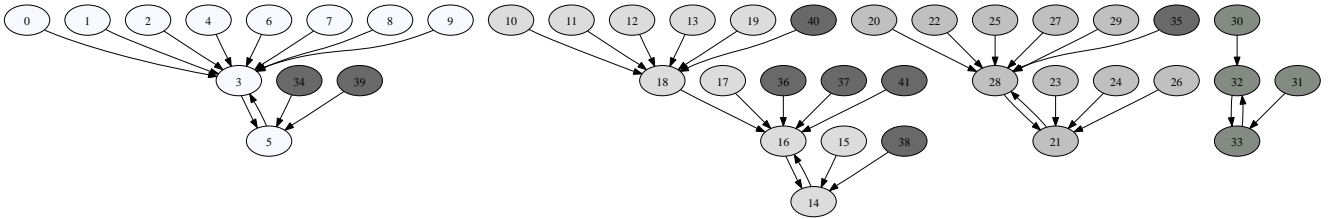


FIG. 5: Graphical presentation of clusters at $\tilde{\rho} = 8$. Increasing $\tilde{\rho}$ did not separate the data set (10-19) and (34-41). Instead they together make one big cluster.

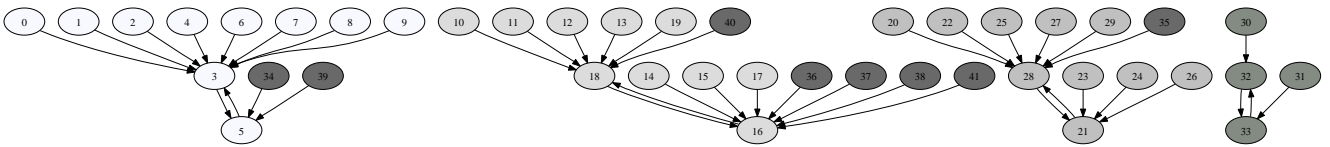


FIG. 6: Graphical presentation of clusters at $\tilde{\rho} = 10$. Though still we have four clusters, second cluster from the left has compactified.

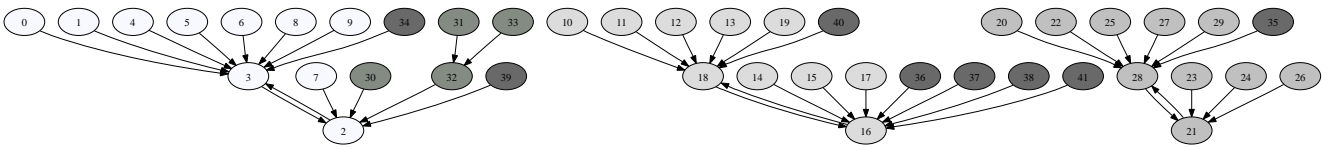


FIG. 7: Graphical presentation of clusters at $\tilde{\rho} = 15$. At this point, the clusters (0-9) and (30-33) have merged together, suggesting a closeness among them relative to other clusters.

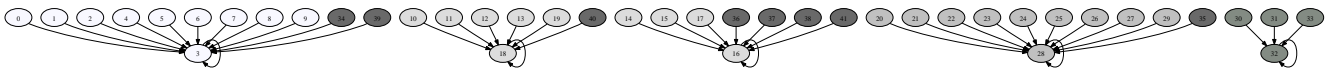


FIG. 8: Graphical presentation of clusters in the limit of $\tilde{p} \rightarrow \infty$. Here, unlike the above figures, all the information about the hierarchical structure is lost. Hence it is almost impossible to deduce the sources of error from this clustering.

D. SRBCT cancer data

This set has 63 samples with 2308 genes and 4 expression diagnosis patterns [14].

For \tilde{p} going to infinity, the best tuning-robust estimates groups cluster data into 5 clusters making as many as 22 errors. On the other hand, with finite \tilde{p} , SCAP finds a regime of 4 clusters, making only 7 assignment errors. Here, Dettling reports only 1.24% generalization error in supervised classification, corresponding to less than one error on 63 patterns. Classification thus performs considerably better than clustering alone.

E. Leukemia

This set has 72 samples with 3571 genes and 2 expression patterns [15].

In the case of infinite \tilde{p} , the original AP groups data into 2 clusters with 4 errors, while for variable \tilde{p} (fixing σ very large) modified AP finds 2 clusters with 2 errors. Also classification leads to 2.5% of errors, a result which is slightly better than our clustering result.

IV. METHODS

In the process of choosing exemplars, we are interested in calculating marginals

$$P_\mu(c_\mu) = \sum_{\{c_\nu\}_{\nu \neq \mu}} P(c) \quad (8)$$

$P_\mu(c)$ is the probability that data point μ chooses point c as its exemplar. The calculation of marginals can be done iteratively via a message passing algorithm called Belief Propagation (BP). BP is based on a variational minimization principle [9] exact on tree factor graphs but usable heuristically in the general case. Together with a generalized larger family of message passing algorithms, it was proven to be very powerful in solving NP-hard combinatorial problems on diluted, tree-like structures, under some general assumptions that go under the name of *cavity method* in statistical physics [17, 18]. Recently, the validity of the cavity approach and in particular the use of BP approximation was also shown to be efficient in some important problems giving rise to dense and very loopy factor graphs [16, 19]. In this framework, both AP and SCAP use BP as an heuristic approach to compute quantities (8).

Looking at figures (9) and (10), the BP algorithm computes marginal probabilities $P_\mu^{BP}(c)$ as products of messages $A_{\lambda \rightarrow \mu}(c)$ coming from each compatibility constraint, times the local prior computed as the exponential of a field which measures the strength of the known similarity between point μ and its putative exemplar c . Up to an overall normalization constant, we can write:

$$P_\mu^{BP}(c) \propto \prod_\lambda A_{\lambda \rightarrow \mu}(c) e^{\beta S(\mu, c)} \quad (9)$$

where β plays the role of an annealing parameter measuring the relative importance given to the priors compared to the internal messages passed information. Messages $A_{\lambda \rightarrow \mu}(c)$ can be interpreted, if normalized, as the probability that μ chose c as its exemplar if in presence of constraint λ alone, in the BP scheme. Such messages can be calculated via the following self-consistent equations

$$A_{\mu \rightarrow \nu}(c) = \frac{1}{Z_{\mu \rightarrow \nu}^A} \sum_{\{c_\lambda\}} \prod_{\lambda \neq \nu} B_{\lambda \rightarrow \mu}(c_\lambda) \chi_\mu^{(p)}(\{c_\lambda\}, c) \quad (10)$$

$$B_{\mu \rightarrow \nu}(c) = \frac{1}{Z_{\mu \rightarrow \nu}^B} \prod_{\lambda \neq \nu} A_{\lambda \rightarrow \mu}(c) \exp(\beta S(\mu, c)) \quad (11)$$

where the N^2 functions $B_{\mu \rightarrow \nu}(c)$ (same as the number of messages) can be interpreted as probabilities that, in the cavity approximation, data point μ chooses c to be its exemplar in a data set where point ν has been excluded from the calculation. These probabilities are called *cavity probabilities*, because the disregarding of one data point effectively carves a cavity in the original factor graph. Quantities $Z_{\mu \rightarrow \nu}^A$ and $Z_{\mu \rightarrow \nu}^B$ are normalization factors defined by enforcing $\sum_c A_{\mu \rightarrow \nu}(c) = \sum_c B_{\mu \rightarrow \nu}(c) = 1 \forall \{\mu, \nu\}$. The *link direction* of functions A s and B s is shown in fig. (9) together with a scheme of the factor graph structure. Fig. (10) shows a pictorial representation of the flow of messages (10) and (11).

Along the lines of [1] and [2], but bearing in mind the slightly modified form for the compatibility constraints, eq. (10) can be simplified after a few manipulations in the following way, depending on cases:

$$\begin{aligned}
(\mu = \nu) \wedge (c = \mu) &\rightarrow A_{\mu \rightarrow \mu}(\mu) = \frac{1}{Z_{\mu \rightarrow \mu}^A} \prod_{\lambda \neq \nu} \sum_{\{c_\lambda\}} B_{\lambda \rightarrow \mu}(c_\lambda) = \frac{1}{Z_{\mu \rightarrow \nu}^A} \\
(\mu = \nu) \wedge (c \neq \mu) &\rightarrow A_{\mu \rightarrow \mu}(c : c \neq \mu) = \frac{1}{Z_{\mu \rightarrow \mu}^A} [p + (1-p) \prod_{\lambda \neq \nu} (1 - B_{\lambda \rightarrow \mu}(\mu))] \\
(\mu \neq \nu) \wedge (c = \mu) &\rightarrow A_{\mu \rightarrow \nu}(\mu) = \frac{1}{Z_{\mu \rightarrow \nu}^A} [p + (1-p) B_{\mu \rightarrow \mu}(\mu)] \\
(\mu \neq \nu) \wedge (c \neq \mu) &\rightarrow A_{\mu \rightarrow \nu}(c : c \neq \mu) = \frac{1}{Z_{\mu \rightarrow \nu}^A} [p + (1-p) ((B_{\mu \rightarrow \mu}(\mu)) + \prod_{\lambda \neq \nu} (1 - B_{\lambda \rightarrow \mu}(\mu)))]
\end{aligned} \tag{12}$$

with

$$Z_{\mu \rightarrow \mu}^A = 1 + (N-1) [p + (1-p) \prod_{\lambda \neq \nu} (1 - B_{\lambda \rightarrow \mu}(\mu))] \tag{13}$$

$$\begin{aligned}
Z_{\mu \rightarrow \nu}^A &= p + (1-p) B_{\mu \rightarrow \mu}(\mu) + \\
&(N-1) [p + (1-p) (B_{\mu \rightarrow \mu}(\mu) + \prod_{\lambda \neq \nu} (1 - B_{\lambda \rightarrow \mu}(\mu)))]
\end{aligned} \tag{14}$$

It is remarkable that the number of effectively independent quantities present in Eqs. (10) is much smaller than the apparent $O(N^3)$ real valued numbers. Indeed, functional messages A take only 2 different values: $A_{\mu \rightarrow \nu}(\mu)$, that from now on will be called $A(\nu, \mu)$ to avoid index redundancy, and $A_{\mu \rightarrow \nu}(c : c \neq \mu) = \hat{A}_{\mu \rightarrow \nu}$ independently on c , as long as it is $\neq \mu$. The exchange of indexes in $A(\mu, \nu)$ is pure convention, but it has been introduced for coherency with the definition of availabilities given in [1]. It follows immediately from the normalization condition that $\hat{A}_{\mu \rightarrow \nu} = (1 - A(\nu, \mu)) / (N - 1)$.

For the cavity probability functions, manipulation of Eq. (11) involving the use of the last normalization condition and of the normalization constant rescaling, leads to

$$\begin{aligned}
(\mu = \nu) \wedge (c = \mu) &\rightarrow B_{\mu \rightarrow \mu}(\mu) = R(\mu, \mu) = \frac{e^{\beta S(\mu, \mu)}}{Z_{\mu \rightarrow \mu}^B} \\
(\mu = \nu) \wedge (c \neq \mu) &\rightarrow B_{\mu \rightarrow \mu}(c : c \neq \mu) = \frac{1}{Z_{\mu \rightarrow \mu}^B} \frac{(N-1) A(\mu, c) e^{\beta S(\mu, c)}}{1 - A(\mu, c)}
\end{aligned} \tag{15}$$

$$(\mu \neq \nu) \wedge (c = \mu) \rightarrow B_{\mu \rightarrow \nu}(\nu) = R(\mu, \nu) = \frac{e^{\beta S(\mu, \nu)}}{Z_{\mu \rightarrow \nu}^B} \tag{16}$$

$$(\mu \neq \nu) \wedge (c \neq \nu) \rightarrow B_{\mu \rightarrow \nu}(c : c \neq \nu) = \frac{1}{Z_{\mu \rightarrow \nu}^B} \frac{(N-1) A(\mu, c) e^{\beta S(\mu, c)}}{1 - A(\mu, c)}$$

with

$$Z_{\mu \rightarrow \nu}^B = e^{\beta S(\mu, \nu)} + (N-1) \sum_{c: c \neq \nu} \frac{A(\mu, c) e^{\beta S(\mu, c)}}{1 - A(\mu, c)} \tag{17}$$

Messages $B_{\mu \rightarrow \nu}(\nu) \rightarrow R(\mu, \nu)$ have been also renamed with a symbol coherent with the *responsibility-availability* notation of [1]. It can be seen that self consistent equations close into the $O(N^2)$ quantities $A(\nu, \mu)$ and $R(\mu, \nu)$

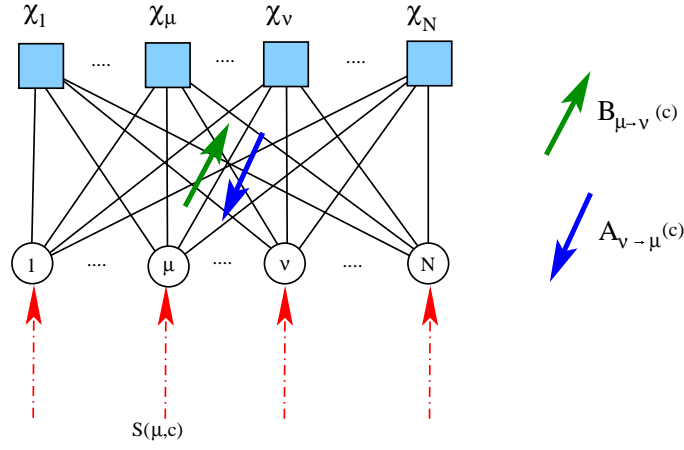


FIG. 9: AP factor graph and direction of sent messages.

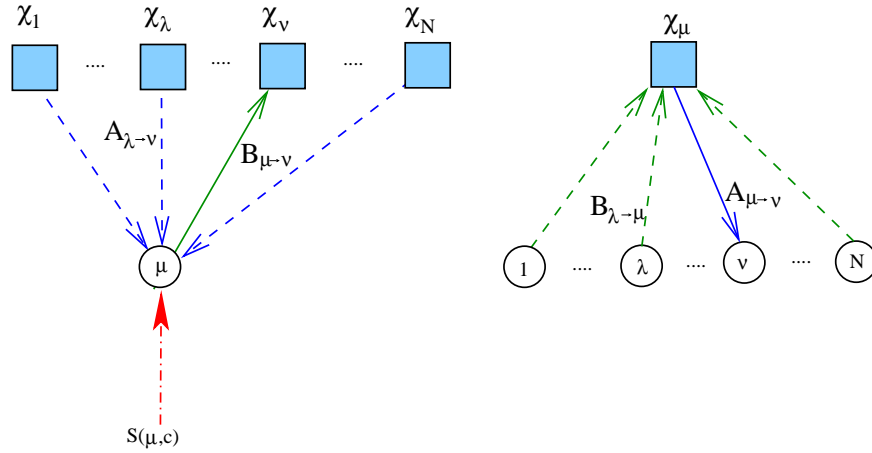


FIG. 10: Pictorial representation of messages flow.

alone. Indeed, the effective dependence on the exemplar choice is dropped, and the computational size of the problem reduces by a factor N . The set of equations of A and R can be solved iteratively via the BP algorithm. The case in which one is interested not in the whole form of the posterior probability function, but only in retaining information about the most probable exemplar chosen by each data point, can be seen to be equivalent to taking the $\beta \rightarrow \infty$ limit where availabilities a and responsibilities r are introduced in the following way:

$$A(\mu, \nu) = e^{\beta a(\mu, \nu)} e^{\beta \hat{a}_{\nu \rightarrow \mu}} \quad (18)$$

$$\hat{A}_{\nu \rightarrow \mu} = e^{\beta \hat{a}_{\nu \rightarrow \mu}} \quad (19)$$

$$R(\mu, \nu) = e^{\beta r(\mu, \nu) + \beta \max_{c: c \neq \nu} \{r_{\mu \rightarrow \nu}(c: c \neq \nu)\}} \quad (20)$$

$$B_{\mu \rightarrow \nu}(c: c \neq \nu) = e^{\beta r_{\mu \rightarrow \nu}(c: c \neq \nu)} \quad (21)$$

and treating the exponential scaling in a regime where prior similarities between data points S are of the same order of magnitude of the value of a and r . The rescaling of responsibilities can be freely done as it does not change the number of independent variables. From the last definitions one is led to equations

$$A(\mu, \nu) = \frac{1}{1 + (N-1)e^{-\beta a(\mu, \nu)}} \quad (22)$$

$$R(\mu, \nu) \sim \frac{1}{1 + e^{-\beta r(\mu, \nu)}} \quad (23)$$

where the last relation already implies a large β behavior in the hypothesis of non degeneracy of the most probable value of the cavity probabilities. This hypothesis is equivalent to having non-degenerate choices of exemplars for

all data points, i.e., to the existence of a single optimal clustering identified via the SCAP algorithm as the unique ground state of the system energy (4). This is a sensible assumption, but it is not always satisfied in interesting cases. Studying the degenerate number and behavior of clustering choices is another crucial question that is only partially answered by the introduction of the relaxation parameter p and will be the subject of further work beyond this paper. In the large β regime, in order to work with quantities all with the same scaling, it is useful to define

$$p = e^{-\beta\tilde{p}} \quad (24)$$

and consider \tilde{p} , a and r fixed varying β . Equating Eqs. (22) and (23) with Eqs. (12) and (16) respectively, and extracting the leading terms in the large β limit assuming no degeneracy, the following equations are found, using Eq. (24):

$$\begin{aligned} r(\mu, \nu) &= S(\mu, \nu) - \max_{\lambda \neq \nu} [S(\mu, \lambda) + a(\mu, \lambda)] \\ r(\mu, \mu) &= S(\mu, \mu) - \max_{\lambda \neq \mu} [S(\mu, \lambda) + a(\mu, \lambda)] \\ a(\mu, \nu) &= \min \left[0, \max(-\tilde{p}, \min(0, r(\nu, \nu))) + \sum_{\lambda \neq \mu} \max(0, r(\lambda, \nu)) \right] \\ a(\mu, \mu) &= \min \left[\tilde{p}, \sum_{\lambda \neq \mu} \max\{0, r(\lambda, \mu)\} \right]. \end{aligned} \quad (25)$$

Making another change of variables redefining the self-responsibilities as

$$r'(\mu, \mu) = \max[-\tilde{p}, r(\mu, \mu)] - \max_{\mu} \{r(\mu, \mu)\} \rightarrow r(\mu, \mu) \quad (26)$$

we get, in terms of the rescaled quantities,

$$\max(-\tilde{p}, \min(0, r(\mu, \mu))) = r(\mu, \mu) \quad (27)$$

leading to SCAP equations (6)[22]. After convergence, marginals can be written [1, 9] as

$$\begin{aligned} P_{\mu}(c) &\sim P_{\mu}^{BP}(c) \propto \prod_{\lambda} A_{\lambda \rightarrow \mu}(c) \exp(\beta S(\mu, c)) \\ &\propto R(\mu, c) A(\mu, c) \propto e^{\beta(a(\mu, c) + r(\mu, c))} \end{aligned} \quad (28)$$

In the $\beta \rightarrow \infty$ limit, one can write equation (7).

V. DISCUSSION

Affinity Propagation is a new powerful tool for unsupervised clustering. It has many very strong points. First it is very efficient, convergence to the final clustering is very fast, the latter appears to be independent on the initialization of messages. Second, due to its hard constraints AP identifies exemplars which are prototypical data points representing a whole cluster.

This last point is, however, also a first limitation of the original AP algorithm. If clusters cannot be well-represented by a single cluster exemplar, AP has to fail. The hard constraint renders the algorithm greedy, and small fluctuations in the similarity measure may trigger avalanches in the exemplar choice leading to different clusterings for only slightly modified model parameters.

We have introduced a soft-constraint version of affinity propagation which is able to cure a part of these problems without losing the efficiency of the original AP:

- By relaxing the hard constraint on clusters exemplars, we could introduce a parameter (\tilde{p}) controlling the algorithm greediness. \tilde{p} is a better tuning parameter than σ (it is more informative and leads to more robust and stable clustering) and it is easier to interpret the statistical meaning of its tuning process.
- Clusters are more robust than in the original formulation of the algorithm. Moreover, even though a second *a priori* free-parameter is introduced, the overall dependence of the algorithm on free parameters is reduced, and an optimal tuning strategy naturally emerges.
- The cluster structure can be efficiently probed. This concerns the internal structure of the clusters since SCAP is able to identify central and peripheral nodes of each clusters, as well as the hierarchical organization leading to a process of cluster merging if cluster number is reduced by looking to less fine structures.

We conclude therefore that SCAP is more efficient than AP in particular in the case of noisy, irregularly organized data - and thus in biological applications concerning microarray data. The computational efficiency of SCAP allows there to treat also very large data sets.

Acknowledgments

We acknowledge very useful discussions with Alfredo Braunstein, Andrea Pagnani and Riccardo Zecchina, and we are grateful to M. Dettling for making his preprocessing of the used microarray data publicly available. M.L. would like to thank the Malawi Polytechnic for hospitality during the preparation of the manuscript. The work of S. and M.W. was supported by the EC via the STREP GENNETEC (“Genetic networks: emergence and complexity”).

-
- [1] Frey, J.F. and Dueck, D. (2007) Clustering by Passing Messages Between Data Points, *Science* **315**, 972-976.
- [2] Frey, J.F. and Dueck, D. (2007) Mixture Modeling by Affinity Propagation, freely available at books.nips.cc/papers/files/nips18/NIPS2005_0799.pdf
- [3] Jain, A.K., Murty, M.N., and Flynn, P.J. (1999) Data Clustering: A Review, *ACM Computing Surveys*, **31**, 264-323.
- [4] MacQueen, J., *Proc. Fifth Berkeley Symp. on Mathematical Statistics and Probability*, L. Le Cam, J. Neyman, Ed. (Univ. of California Press 1967), 281.
- [5] Shi, J., Malik, J., (2000) *IEEE Trans. Pattern Anal. Mach. Intell.* **22**, 888.
- [6] Blatt, M., Wiseman, S. and Domany, E. (1996) Super-paramagnetic clustering of data, *Physical Review Letters*, **76**, 3251.
- [7] Shental, N., Zomet, A., Hertz, T. and Weiss, Y. (2003) Pairwise Clustering and Graphical Models, *17th Int. Conf. on Neural Information Processing Systems - NIPS*, Vancouver, Canada, December 2003.
- [8] Duda, R. O. and Hart, P. E., *Pattern Classification and Scene analysis* (Wiley, New York 1973).
- [9] Yedidia, J.S., Freeman, W.F., and Weiss, Y. (2005) Belief Propagation and Generalizations, *IEEE Trans. Inform. Theory* **51**, 2282.
- [10] F. R. Kschischang, B. J. Frey, H.-A. Loeliger, (2001) Factor Graphs and the Sum-Product Algorithm, *IEEE Trans. Inform. Theory* **47**, 1.
- [11] Pomeroy, S., Tamayo, P., Gaasenbeek, M., Sturla, L., Angelo, M., McLaughlin, M., Kim, J., Goumnerova, L., Black, P., Lau, C. et al. (2002). Prediction of Central Nervous System Embryonal Tumor Outcome Based on Gene Expression. *Nature* **415**, 436-442.
- [12] Dettling, M. (2004), BagBoosting for Tumor Classification with Gene Expression Data, *Bioinformatics* **20**, 3583-3593.
- [13] Alizadeh, A., Eisen, M., Davis, R., Ma, C., Lossos, I., Rosenwald, A., Boldrick, J., Sabet, H., Tran, T., Yu, X. et al. (2000) Distinct types of diffuse large B-Cell-Lymphoma Identified by Gene Expression Profiling, *Nature* **403**, 503-511.
- [14] Khan, J., Wei, J., Ringner, M., Saal, L., Ladanyi, M., Westermann, F., Berthold, F., Schwab, M., Antonescu, C. et al. (2001) Classification and Diagnostic Prediction of Cancer Using Gene Expression Profiling and Artificial Neural Networks. *Nature Medicine* **6**, 673-679.
- [15] Golub, T., Slonim, D., Tamayo, P., Huard, C., Gaasenbeek, M., Mesirov, J., Coller, H., Loh, M., Downing, J. et al. (1999) Molecular Classification of Cancer: Class Discovery and Class Prediction by Gene Expression Monitoring. *Science* **286**, 531-537.
- [16] Braunstein, A., Zecchina, R. (2006) Learning by Message passing in Networks of Discrete Synapses *Phys Rev. Lett.* **96** 030201.
- [17] Mézard, M., Parisi, G., Zecchina, R. (2002) Analytic and Algorithmic Solution of Random Satisfiability Problems, *Science* **297**, 812.
- [18] Hartmann, A.K., Weigt, M. (2005) *Phase Transitions in Combinatorial Optimization Problems* (Wiley-VCH, Berlin 2005).
- [19] Kabashima, Y. (2003) A CDMA multiuser detection algorithm on the basis of belief propagation, *J. Phys. A* **36**, 11111-11121.
- [20] Other limitations may lie in the choice of a non optimal similarity function, or in the pairwise nature of the interaction that does not take into account that the similarity between two data points could be dependent on the presence or absence of other points in the data set. This would result in an effective many-body similarity function. However, these effects are not easily measured in raw biological data and/or imply some degree of prior knowledge of the sought clustering solution, which is usually not available in unsupervised clustering schemes like the one implemented via the AP algorithm.
- [21] Prior biological knowledge leading to a preference of some data points to be exemplars may be implemented via a non-homogeneous self-similarity.
- [22] Note that the last change of variable via the subtraction of the overall quantity $\max_{\mu} \{r(\mu, \mu)\}$ is redundant if self responsibilities are negative, as it is usually the case.